Final Technical Report
Grant N00014-97-1-G024

"Tuning And Aging Characteristics of Multi-Section Wide Wavelength Tunable Semiconductor Lasers"

Daniel J. Blumenthal
Optical Communications and Photonic
Networks (OCPN) Laboratory
Department of Electrical and Computer Engineering
University of California, Santa Barbara, CA 93106
Tel: (805) 893-4168
Fax: (805) 893-5705

Email: danb@ece.ucsb.edu

Executive Summary

This final report summarizes progress on analysis of wavelength tuning characteristics under accelerated aging lifetime measurements. This work involved design and construction of a 10-laser lifetime testbed that measures, under computer control, different wavelength based characteristics at elevated temperatures over a period of 5000 hours. A detailed static and dynamic model for simulation of GCSR lasers was developed and used to analyze lasers behavior.

Objectives

To quantify and analyze the various wavelength tuning aging characteristics of Altitun GCSR tunable semiconductor lasers. To measure the wavelength characteristics of the tunable lasers using accelerated lifetime aging by maintaining the tunable laser at 50 and 65° C and automate the data collection of the characteristics over 5000 hrs. To identify physical aging mechanisms and relate them to fabrication, estimate realistic lifetime of devices, quantify and analyze various changes in output/tuning characteristics of devices, identify physical aging mechanisms and relate back to fabrication. To develop analytical model in order to study static and dynamic GCSR laser wavelength tuning, as well as switching times.

Purchased Equipment

The following equipment was purchased in conjunction with industrial matching funds in the form of discounts greater than the standard educational discounts.

Vendor/	(Qnty)	Description	Cost
Altitun	(10)	Packaged tunable 4-section semiconductor lasers from IMC	$128,200.95
Dell Computer Corp	(2)	Computers	$5501.40
Hewlett Packard Company/			
	(1)	Signal Generator	
	(1)	High –Stability Time Base	
	(1)	Rear Panel Connector	
	(1)	Enhanced Spectral Purity	
Photonetics	(1)	WALICS/Multi-Wavelength Analyzer	$38359.00
JDS Fitel Lightwave	(1)	Optical Amplifier Module with optical isolators and FC/PC Contact	$8943.93
Total Purchase Cost for all Items			**$212,167.45**

Introduction

Widely-tunable GCSR lasers are one of the most promising candidates for applications in future optical networks. However, for system applications, requirements on the reliability of the device are very stringent. In order to ensure wavelength agility and failure-free operation, wavelength tunable devices must not only achieve wide wavelength tuning ranges, but also support stable single-mode operation with high output power and high SMSR for each of these wavelength channels during the operating lifetime of the device (10-20 years). Lasing wavelength, power and corresponding currents of the device should ideally operate in a "set-and-forget" mode i.e. a specific wavelength should always be accessible with the same values of injected currents. Furthermore, different channels should not exhibit frequency fluctuations, unwanted mode-hops or overlap. Thus, reliability and aging studies are necessary to define stability of these lasers and their expected lifetime in the network.

There are multiple potential reasons for a laser to change its output characteristics (age). The most common causes together with their aging effect are listed in Table 1.

Table 1. Most common causes and aging effects in lasers.

Cause	Aging Effect
growth of material defects	non-radiative recombination centers
degradation of overgrown grating interface	non-radiative recombination centers
facet and reflection coating degradation	reduction of light output
contact and bonding degradation	increased thermal impedance
fiber misalignment	reduction of light output
temperature sensor/Peltier cooler degradation	temperature instability within the package
accumulation of package water contents	risk of corrosion

In this study we do not address such issues as contact and bonding degradation, Peltier cooler degradation or accumulation of water inside the package. This study is intended to identify and quantify the changes related to the changes in output power or lasing wavelength which could be more likely caused by degradation of overgrowth interfaces or laser facet degradation.

Experimental Description

The schematic structure and measured lasing spectra at different ITU grid channels are shown in Figure 1. Device fabrication and tuning mechnisms of these lasers has been described elsewhere [1,2,3]. GCSR lasers can be made to operate at any of the desired channels with ±10MHz accuracy by proper setting of the coupler, reflector and phase sections currents. During the reported accelerated aging test, the lasing frequency, power and SMSR ratio for a large number of channels within each device were systematically measured and recorded after a given regular period of time. A preliminary 37 hour burn-in at 85°C eliminated infant defect devices, and no critical failures were observed during the performed test.
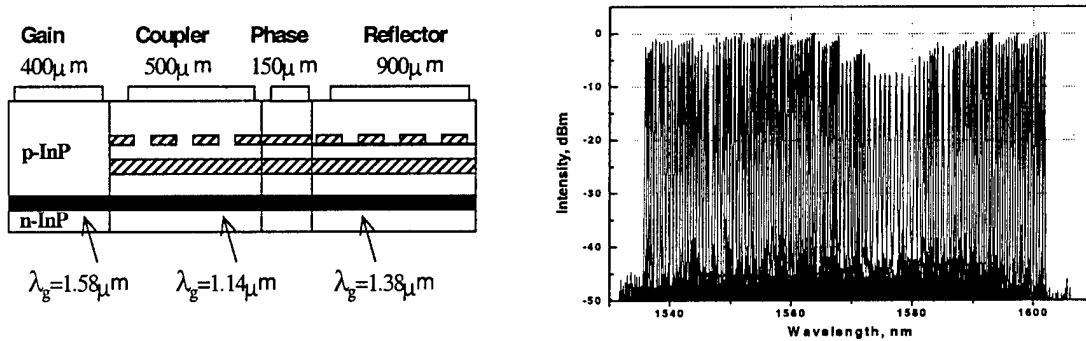
Figure. 1: (a) Schematic structure of the Grated Coupler Sampled Reflector (GCSR) laser
(b) Superimposed optical spectra of a large number of ITU channels spaced 50 GHz apart

A schematic of the lifetime characterization testbed is illustrated in Figure 2. The testbed is designed to measure tunable laser characteristics in an accelerated aging environment. These characteristics include the wavelength tuning repeatability and wavelength vs.

current tuning curve, the output power as a function of wavelength, laser threshold as a function of wavelength, Sidemode Suppression Ratio (SMSR) as a function of wavelength and laser linewidth as a function of wavelength. Lasers are continuously operated at maximum currents and laser characteristics are measured in a regular periods of time. The whole procedure is governed by a computer-based code (currently "LabView" code). Shown in Figure 1 are from top to bottom, the computer for measurement control and data acquisition. Acquisition is performed using GPIB while laser control is performed through an RS232 bus. An uninterrupted power supply (UPS) is used to prevent data and laser loss during power outages, brownouts and spikes. An internal 1 Gbyte removable media cartridge is used for scheduled data backup. The lasers are housed in a 10-laser mainframe. Each laser is mounted in a butterfly package on a PC board. Each PC board has a controller that sets currents for 4 laser sections and the temperature of the laser package. These parameters are controlled using RS232 commands at the board input. The mainframe provides power to the 10 boards as well as a switched RS232 bus to allow communications to any laser using only one RS232 connection to the computer. Optical characteristics are measured by using a 1x12 optical switch to connect one laser at a time (under computer control) to the optical spectrum analyzer. A photograph of the lifetime characterization testbed is shown in Figure 3. A close-up of a single channel Altitun GCSR laser module for the 10-card mainframe is shown in Figure 4. Current control for each of 4 sections of each laser and temperature control is performed by onboard circuitry controlled through the RS232 mainframe bus.

Table 2 summarizes the conditions of the accelerated aging measurements. The first short (600 hour long) test was intended to study the changes in early device operation. Major changes happened within the first few hundred hours following burn-in, with only much smaller changes occuring during further operation of the device. Similar changes were observed previously [8]. This behavior suggests that a second longer burn-in of the devices that have passed the infant death and defects screening should be
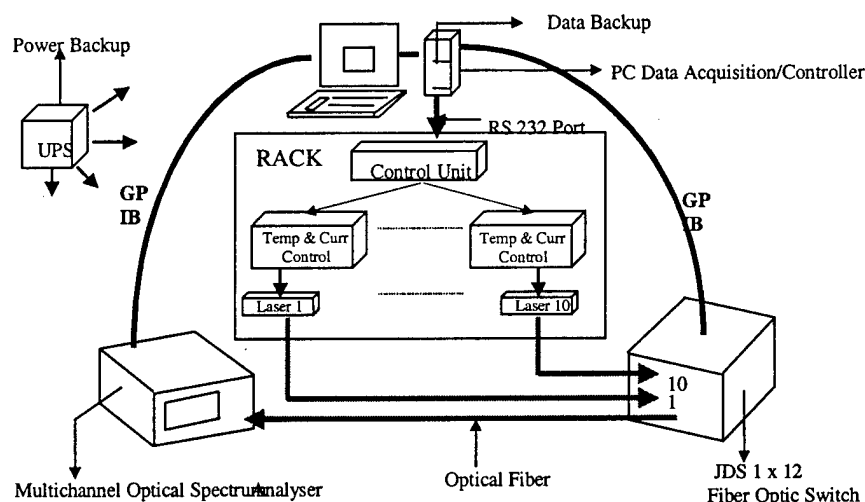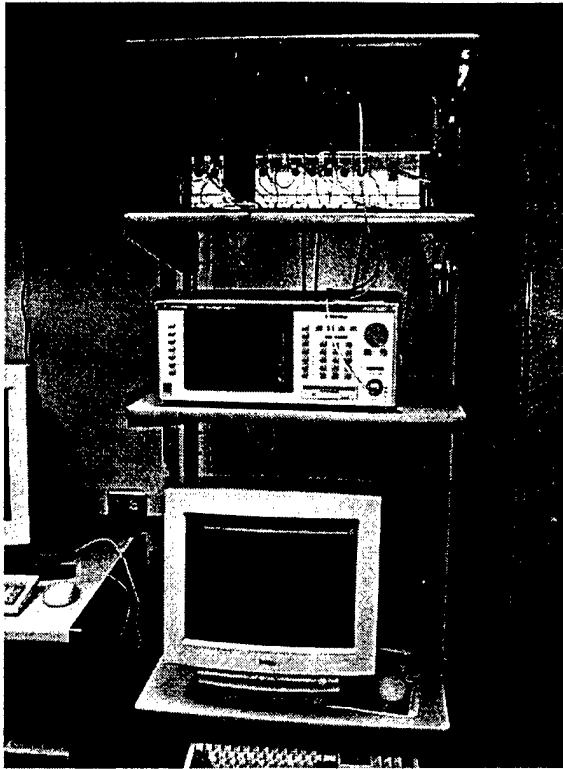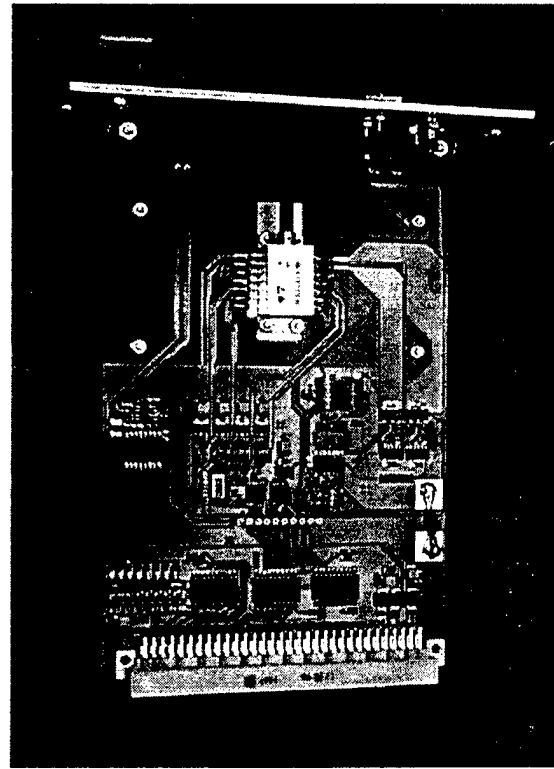

Figure 2. Schematic of tunable laser accelerated aging testbed.

Figure 3. Photograph of laser aging characteristic testbed.

Figure 4. Closeup view of GCSR laser module.

Table 2. Conditions of the performed accelerated aging tests.

| Test number	Number of devices	Number of ITU channels	Aging Currents, mA (Gain, Coupler, Reflector, Phase)	Aging Temperature, °C	Duration, hours	Test Objectives
1	1	96	(150,15,15,5)	50, 60	600	Study early changes; define appropriate burn in time
2	4	168	(150,15,15,5)	50	3000	Wavelength, power SMSR
3	4	322	(150,15,15,5)	65	3000	and current stability device operation lifetime

employed to ensure stability before they go into the network. This will be discussed in more detail later.

Further, eight randomly selected devices were operated continuously at 50 and 65°C for 3000 hours (see Table 2) and their characteristics were recorded at set intervals of time. Aging currents of the Gain, Coupler, Reflector and Phase sections were set to 150, 15, 15 and 5 mA correspondingly which are the maximum currents normally needed to obtain the full tuning range of the laser.

Measurement Results and Discussion

Figure 5(a) shows measured frequencies of channels within one device as a function of aging time. It can be seen that that some channels are stable and remain at their orginal frequencies even after a long operation time at elevated temperature, but there are a number of channels that experience spontaneous mode hopping to a new frequency location.

Under closer inspection it turns out that it is not only mode hopping that channels can experience, but also a gradual frequency shift as operation time increases. Figure 6(a)
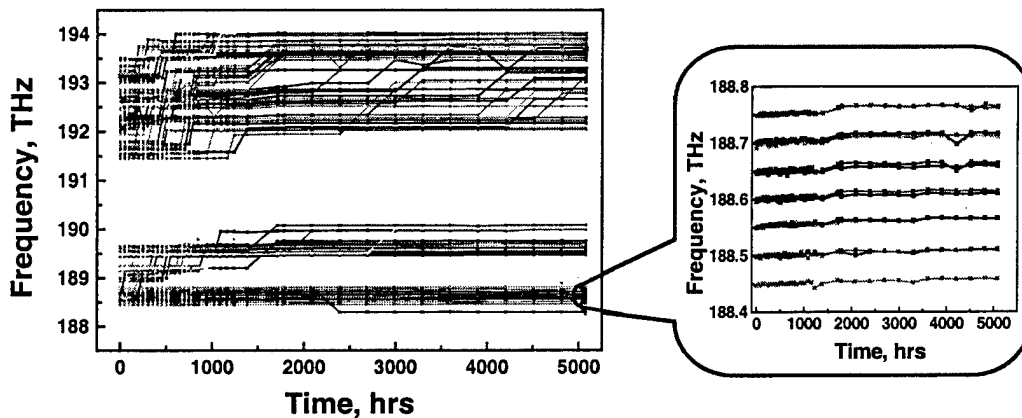
Figure 5. Measured frequencies of 96 channels within one device as a function of aging time.

shows normalized frequency shifts for the stable channels. It can be seen that most of the changes take place during first 50-200 hours of device operation. There is a significant spread in the amount of the final shift - between 20 and 50 GHz. However, a major
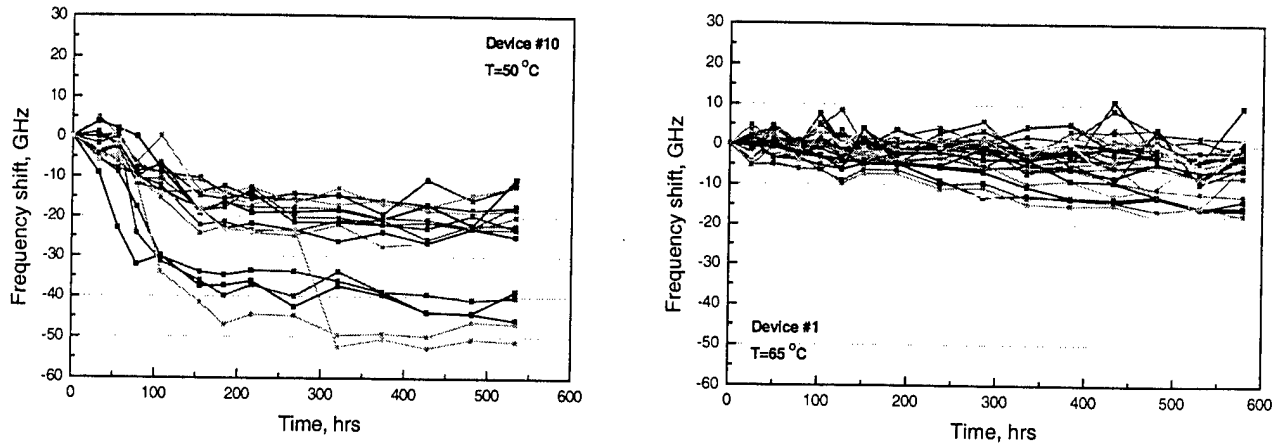

Figure 6. Normalized frequency shifts as a function of aging time for :
(a) device with only 37 hours burn-in; (b) device with a 37 and 600 hours burn-ins

improvement in the frequency stability may be obtained if a device is given an additional burn-in prior to the actual operation time. Figure 6(b) shows normalized frequency shift for a similar device that had a 600 hour burn-in (as in test 1, Table 1) prior to the aging test. Frequency shifts for this device are significantly smaller – between 2 and 20 GHz. It is important to notice that the channels exhibiting larger frequency shifts correspond to the shorter wavelengths, obtained with higher tuning currents. This means that frequency drift is non-uniform over the spectral range and a function of the tuning current magnitude.

While gradual frequency shifts are most likely due to heterointerface degradation and increasing leakage currents, the origin of the large jumps in frequency (as in Fig. 5) can be understood if we analyze the changes of tuning properties of the device with operation time. Figure 7 shows wavelength tuning curves as a function of coupler current (coarse tuning). It can be seen that as operation time increases, constant wavelength plateaus are shifting to smaller current values. This means that given the same value of injected current, the lasing wavelength will hop to the wavelength of the next plateau with increasing time. Since tuning requires three variable currents to obtain lasing at a given ITU frequency, the probability of a wavelength jump increases proportionally. As seen in Figure 7, power stays almost constant throughout the opertaion time, since we can make a conclusion that the most import effect of aging is wavlength (frequency) shift.

The median device lifetime may be found from the log-normal cumulative failure plot. In our study we have chosen the end-of-life criteria to be a 10 GHz shift of the channel frequency from its original position. Such that a device is considered to reach its end of life when 50% of the selected channels exhibit frequency shifts equal or greater than 10 GHz. Figure 8 shows cumulative failure (CF) plots for six devices operated at 50 and 65°C. Two different slopes can be observed on the CF curves, this means that we can dustinguish two different failure mechanisms. The first linear region is related to rapid

changes during initial operation time, it will be eliminated if a proper burn-in is applied. The second linear region is the one that we are interested in and is related to the long-term changes in the laser structure that lead to the frequency drift. As seen fron the Fig. 8, two of the devices operated at 65°C reach 80 and 90% failure points and show a median lifetime of 3800 and 2700 hours correspondingly. Three devices operated at 50°C do not reach a 50% failure point, thus the time at which this point will be reached must be extrapolated. The solid squares symbol line corresponds to the device with additional 600 hrs burn in ("device #1" operated at 65°C), the more stable frequency shift curves for this device were shown in Fig. 6(b). The device shows extremely good time-failure rate characteristics – does not reach a 50% failure point even after 5000 hrs of operation at 65°C. The extrapolated median lifetime for this device is as high as 8700 hours.
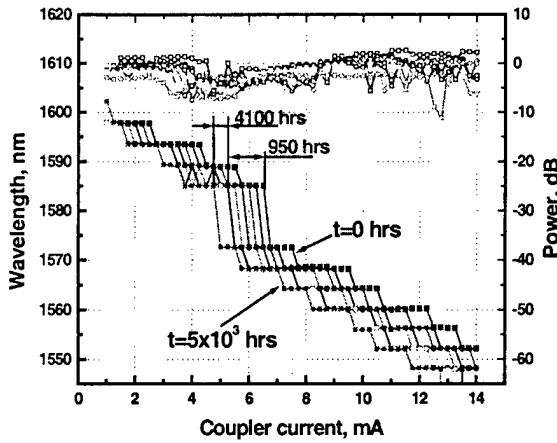

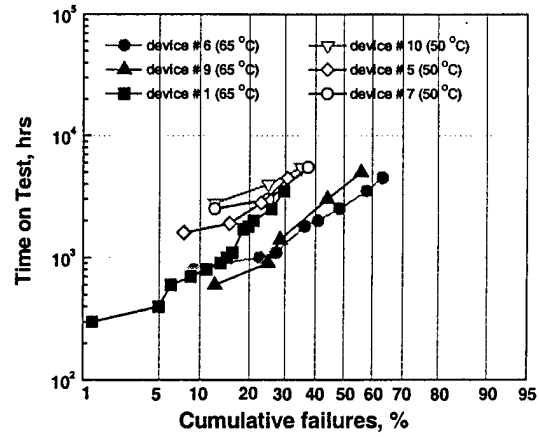*Figure7 . GCSR wavelength tuning curves with laser aging time.*

Figure 8.Log-normal cumulative failures plot.

After the median lifetime at elevated temperatures is found, the Arrhenius equation is used to estimate the median of the device at room-temperature:

$$\frac{\tau(T_1)}{\tau(T_2)} = \exp\left(\frac{E_a}{k}\left(\frac{1}{T_1} - \frac{1}{T_2}\right)\right)$$

where $\tau(T_1)$ and $\tau(T_2)$ are the lifetimes corresponding to the temperatures T_1 and T_2, and E_a is the activation energy. The Arrhenius plot is shown in Fig. 9. The long lifetime point (τ=8700 hrs) at T=65°C corresponds to the above mentioned device with 600 hrs burn-in and will not be taken into account here since it corresponds to a different experiment conditions. The activation energy estimation is 0.68eV and the median lifetime of the device at T=20°C is found to be $117.3 \cdot 10^3$ hours which corresponds to 13.4 years. This lifetime is good enough for the device to be employed in terrestrial optical communication systems and is close to the value required for submarine systems. Also, the device with additional 600 hrs burn-in shows that much longer lifetimes could be achieved with proper burn-in conditions.
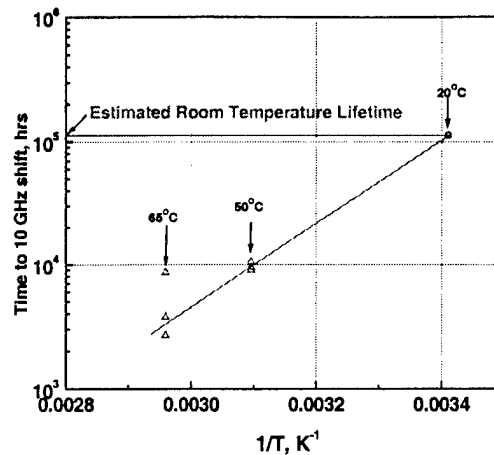
Figure 9. Arrhenius plot for extrapolation of lifetime

Future Work.

We recommend several potential future studies of the tunable laser aging:

1. Perform similar aging study as described in this report on a larger number of lasers (larger sample size). This will comfirm or correct the achieved results as well as verify the activation energy value.

2. Perform a technological study of different aging effects on the laser structure. This is a disctructive type of study, hence will require even larger sample size. However, observing laser strucutre (with such tools as SEM) during different moments of aging history will give direct information the changes.

3. Develop an analytical model describing different processes taking place during the laser aging. Comparing results of modeling of different effects with the experimental results will allow to conclude on major and minor effects and suggest on the ways to improve aging performance.

Aging Study Conclusions.

We have completed a 3000 hour long accelerated aging and reliability study of widely-tunable GCSR lasers. Very stable power and SMSR's were measured, however, lasing frequency drifts were as high as 20-50 GHz. A strong correlation between magnitude of injection current and frequency drift were observed. This can be significantly reduced by an additional burn-in prior to the aging study or application of the device in a real-life system. Equivalent room-temperature lifetime of the device was

estimated to be 11.4 years. A statistical analysis of the observed changes as well as equivalent room temperature operation lifetime, based on the "10 GHz frequency shift" end-of-life criteria was conducted.

Laser Simulation and Modeling Results.

In order to gain better understanding of effects taking place, we have developed a large-signal dynamic model for GCSR lasers. The model is based on the Transfer Matrix Method (TMM) in combination with multi-mode rate equation analysis and takes into account a number of physical processes in the laser cavity such as longitudinal mode spatial hole burning (SHB), non-linear gain compression and refractive index changes with carrier injection.

The basis of the TMM is to divide each laser section longitudinally into a number of sections where the structural and material parameters are assumed to be homogeneous throughout each section as shown in Figure 10. However, these parameters may vary between sections, allowing longitudinal inhomogeneities such as those produced by spatial hole burning to be incorporated into the model. Each of the sections is characterized by its own 2x2 complex transfer matrix that modifies the forward and backward Travelling Wave Amplitudes (TWAs) as they propagate through the section. By calculating TWAs of the electric field and solving the multimode photon rate equation, we can solve for transient and steady state characteristics of the laser. Our goal was to investigate dynamic as well as static tuning behavior of the GCSR laser, i.e. the values of carrier and photon density together with TWAs at each moment of time in each laser subsection. The description of this model and equations used is available in [1].
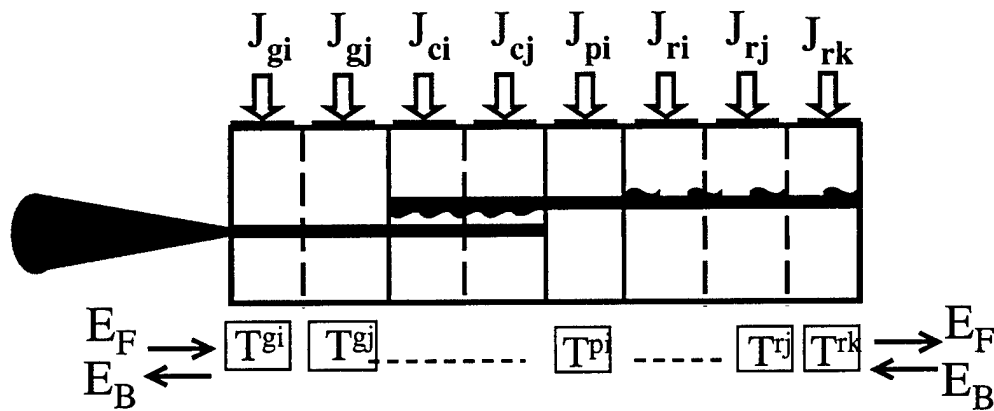

Figure 10. Illustration of the TMM method for simulation of GCSR laser characteristics

Static Tuning. To demonstrate and verify the model, we have performed static analysis of the optical spectra, lasing wavelength and tuning curves of a typical 4 section GCSR laser. The tuning curves of a GCSR laser are an essential point for the comparison

between theory and experiment, since the position and relative amplitudes of various modes are sensitively influenced by the structure and waveguides parameters, the coupling factor, the phase shifts and the unknown end facet phases of the grating. Static tuning curves for the simulated device is shown in the Figure 11(a). It shows the wavelength surface that can be obtained by tuning of the device with both coupler and reflector currents. The peak lasing wavelength is plotted for each pair of coupler and reflector currents with the SMSR ≥ 30 dB criteria, so that no point is plotted in case of multi-mode operation or if the SMSR is less then 30 dB. From the plot we can see that some wavelengths are impossible to obtain or can only be obtained with a poor SMSR - as it can be anticipated, this happens when the Sampled Reflector and Grated Coupler transmission spectras have poor or no overlap. Most of these wavelengths can still be reached when tuning with the phase current is also used. A separate plot would be needed to illustrate this since the phase current would correspond to another dimension.

Figures 11(b) shows experimentally measured tuning curves, similar to the simulated ones in Figure 11(a). Wavelength position of the plateaus are in a good agreement with the simulated ones. A larger number of wavelengths is missing on the measured tuning curve, then it was predicted in the simulation. This may be due to any imperfections of the GCSR fabrication that are difficult to account for in the simulation.
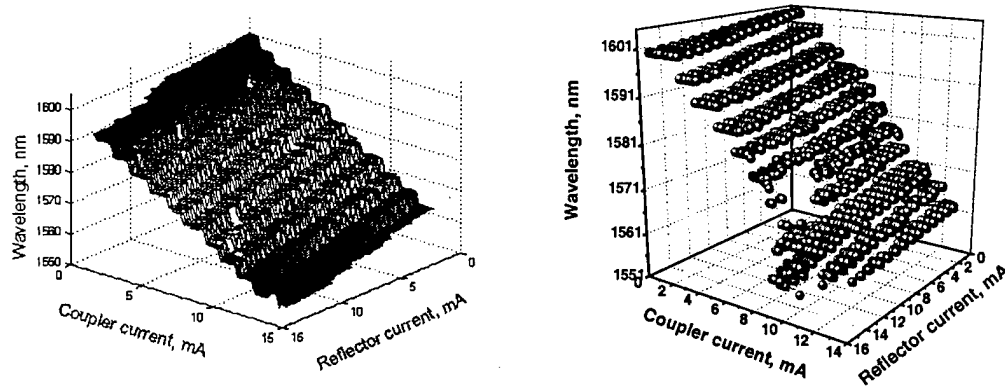

Fig. 11. GCSR wavelength tuning curves (a) calculated and (b) measured

Transient process: Figure 12 shows the calculated transient turn-on process from $I=0mA$ to $I=3I_{th}$ for the two characteristic cases: (a) final state corresponds to a stable single mode operation, and (b) final state corresponds to a multi-mode operation. In the case (a) the peak lasing mode is selected and all other modes are suppressed from the very beginning. Case (b) shows the worst case of the mode competition when both modes come up initially, but the shorter wavelength mode is then slowly suppressed. The side-mode suppression time depends on the initial (zero coupler and zero reflector currents) alignment of the coupler and reflector peaks, which in many cases is determined by the
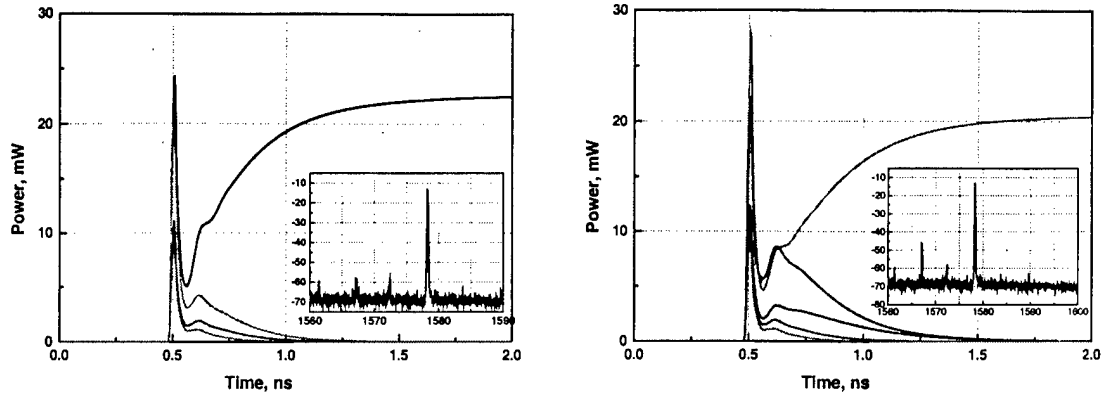
Figure 12. Calculated turn-on process for (a) stable single-mode operation and (b) multi-mode operation cases

unknowns of the technological process (relative phase of the rear facet reflection, phase shift and amplitude of the internal reflections, etc).

Dynamic wavelength switching: Optical network applications require access to a large number of channels and the latency of such networks is determined by the switching time between different channels. Thus it is important to study and optimize the wavelength switching behavior before the laser is employed in a fast optical network. We performed simulations of the wavelength switching between a large number of wavelength channels. The upper curve in Figure 13 shows the simulated waveforms for the case of switching between two different wavelength channels λ_4 and λ_8 which are 20 nm (or three wavelength channels) apart. A significant amount of the interchannel cross-talk noise (momentary spikes of signal at intermediate wavelengths λ_5, λ_6 and λ_7) is observed during the transient time. Simulated waveforms for the same $\lambda_4 \leftrightarrow \lambda_8$ switching but with modified current pulses are shown in the lower waveform in Figure 14. It can be clearly seen that the amount of transient inter-channel crosstalk is much smaller and the switching time is much shorter in this case. Figure 14 shows simulated and measured switching time as a function of a wavelength number for square and differentiated pulses, similar to the one in the Figure 13. The logarithmic increase of the switching time is observed in both cases as the wavelength step increases. However, using the pre-distortion differentiated pulses, we could measure a significant reduction of the switching time. The measured and calculated switching times show a good agreement demonstrating the validity of the proposed dynamic model.
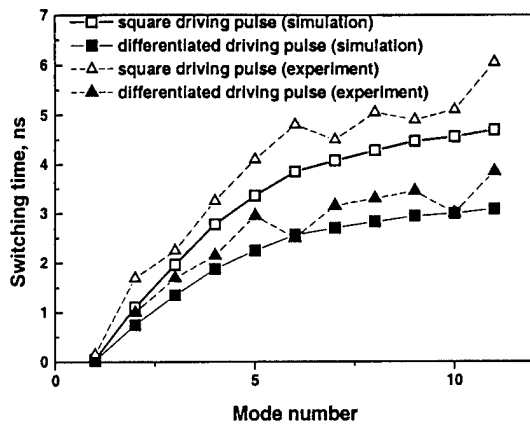
Figure 13. Simulated switching waveforms
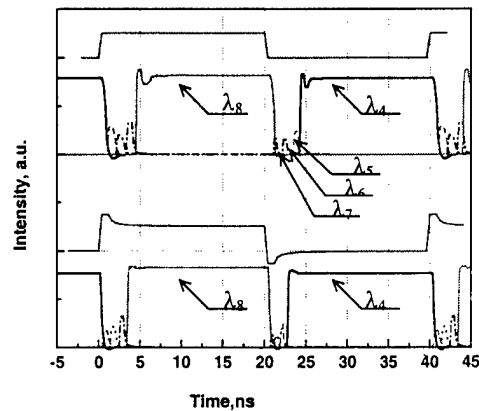for switching between λ_4 and λ_8

Figure 14. Simulated and measured switching time
as a function of wavelength number for square and
differentiated pulses

Personnel Supported

Ph.D. Students: Olga Lavrova, Lavanya Rau,
Masters Students: Scott Humphries
Research Engineer: Laurent Dubertrand
Faculty: Daniel J. Blumenthal

List of Publications

Refereed Journals
1. "Detailed Transfer Matrix Method Based Dynamic Model for Multisection Widely-Tunable GCSR Lasers", Olga Lavrova and Daniel Blumenthal, accepted for publication in *IEEE Journal of Lightwave Technology*, September 2000
2. 2. "Accelerated Aging and Reliability Studies of Multi-Section Tunable GCSR Lasers for Dense WDM Applications", Olga Lavrova and Daniel Blumenthal, submitted for publication in *IEEE Journal of Lightwave Technology* Conference Presentations:Detailed Transfer Matrix Method Based Dynamic Model for Multisection Widely-Tunable GCSR Lasers", Olga Lavrova and Daniel Blumenthal, submitted for presentation at *LEOS'00 Annual Meeting*
2. "Accelerated Aging and Reliability Studies of Multi-Section Tunable GCSR Lasers for Dense WDM Applications", Olga Lavrova and Daniel Blumenthal, *OFC'2000*, paper TuL2, pp. 181-183.
3. "Tuning and Aging Characteristics of Multisection Tunable GCSR Lasers for Dense WDM Applications", *LEOS'99 Annual Meeting*, pp.200-201
4. "Wavelength Tuning Characteristics of the Grated Coupler Sampled Reflector Laser for Wavelength Switching Applications", Olga Lavrova and Daniel Blumenthal, *IPR'99*, paper RMB5-2, pp.20-22

Invention titles

None

Patents applied for

None

Patents issued & patent number

None

Awards received by PI or colleagues/students thru ONR funded work

"ONR Young Investigator Program (YIP) Award"

Technology transitions to industry

None

Technology transitions to other DoD or US Govt Agencies

Lasertest automated computer code sent to NRL for accelerated aging testing of tunable semiconductor lasers, Paul Matthews, 202-767-6324

Number of doctorates awarded

1

Number of masters awarded

1

REPORT DOCUMENTATION PAGE

Public reporting burden for this collection of information is estimated to average 1 hour per response, including the time for reviewing instructions, searching existing data sources, gathering and maintaining the data needed, and completing and reviewing the collection of information. Send comments regarding this burden estimate or any other aspect of this collection of information, including suggestions for reducing this burden, to Washington Headquarters Services, Directorate for Information Operations and Reports, 1215 Jefferson Davis Highway, Suite 1204, Arlington, VA 22202-4302, and to the Office of Management and Budget, Paperwork Reduction Project (0704-0188), Washington, DC 20503.

1. AGENCY USE ONLY (Leave Blank)	2. REPORT DATE	3. REPORT TYPE AND DATES COVERED
	August 29, 2000	Final Technical Report 09/01/97 - 05/31/200

4. TITLE AND SUBTITLE
Tuning and Aging Characteristics of Multisection Wide Wavelength Tunable Semiconductor Lasers

5. FUNDING NUMBERS
N00014-97-1-G024

6. AUTHORS
Daniel J. Blumenthal

7. PERFORMING ORGANIZATION NAME(S) AND ADDRESS(ES)
Department of Electircal & Computer Engineering
University of California, Santa Barbara
Santa Barbara, CA 93106

8. PERFORMING ORGANIZATION REPORT NUMBER

9. SPONSORING / MONITORING AGENCY NAME(S) AND ADDRESS(ES)
Department of the Navy
Naval Research Laboratory
4555 Overlook Avenue, SW
Washington DC 20375-5326

10. SPONSORING / MONITORING AGENCY REPORT NUMBER

11. SUPPLEMENTARY NOTES
The views, opinions and/or findings contained in this report are those of the author and should not be construed as an offiicial Department of the Navy position, policy or decision, unless so designated by other documentation.

12a. DISTRIBUTION / AVAILABILITY STATEMENT

Approved for publi9c release.

12b. DISTRIBUTION CODE

13. ABSTRACT (Maximum 200 words)

This final report summarizes progress on analysis of wavelength tuning characteristics under accelerated aging lifetime measurements. This work involved design and construction of a 10-laser lifetime testbed that measures, under computer control, wavelength based characteristics at elevated temperatures over a period of 5000 hours. A detailed static and dynamic model for simulation of GCSR lasers was developed and used to analyze lasers behavior.

14. SUBJECT TERMS
Tunable lasers, aging characteristics, true time-delay phased array radar

15. NUMBER OF PAGES
14

16. PRICE CODE

17. SECURITY CLASSIFICATION OF REPORT	18. SECURITY CLASSIFICATION OF THIS PAGE	19. SECURITY CLASSIFICATION OF ABSTRACT	20. LIMITATION OF ABSTRACT
UNCLASSIFIED	UNCLASSIFIED	UNCLASSIFIED	UL

NSN 7540-01-280-5500

DTIC QUALITY INSPECTED 4

Standard Form 298 (Rev. 2-89)